Properties of gap junction channels formed of connexin 45 endogenously expressed in human hepatoma (SKHep1) cells

ALONSO P. MORENO, JAMES G. LAING, ERIC C. BEYER, AND DAVID C. SPRAY
Departments of Neuroscience and Medicine, Albert Einstein College of Medicine, Bronx, New York 10461; and Departments of Pediatrics and of Cell Biology and Physiology, Washington University School of Medicine, St. Louis, Missouri 63110

Moreno, Alonso P., James G. Laing, Eric C. Beyer, and David C. Spray. Properties of gap junction channels formed of connexin 45 endogenously expressed in human hepatoma (SKHep1) cells. *Am. J. Physiol.* 268 (*Cell Physiol.* 37): C356–C365, 1995.—We have evaluated the voltage dependence and unitary conductance of gap junctional channels that were recorded in a clone isolated from the hepatoma cell line SKHep1. In this clonal population (designated SKHep1A), Northern blots, immunoprecipitation, and immunohistochemical staining demonstrated the expression of connexin (Cx) 45; no other gap junction protein was identified by these techniques, although weak hybridization with Cx40 was detected. Macroscopic junctional conductance (g_j) in these cells was low, averaging 1.3 nS, and was steeply voltage dependent. Parameters of voltage sensitivity were as follows: voltage at which voltage-sensitive conductance is reduced by 50%, 13.4 mV; steepness of relation, 0.115 (corresponding to 2.7 gating charges), and voltage-insensitive fraction of residual to total conductance $\approx$ 0.06. Unitary conductance (γ_j) of these junctional channels averaged 32 ± 8 pS; although γ_j was independent of transjunctional voltage (V_j), at high V_j values (>50 mV), smaller conductance values were also detected. Open probabilities of the 30-pS channels at various V_j values closely matched the predicted voltage-dependent component of macroscopic g_j; the residual conductance at high V_j might be attributable to the smaller conductance events. The voltage dependence of human Cx45 gap junction channels is as steep as that seen for channels formed by *Xenopus* Cx38 and is much steeper than that previously reported for channels formed of the highly homologous chick Cx45 and for other mammalian connexins expressed either endogenously or exogenously.

single-channel conductance; voltage dependence; connexins; intercellular communication; open probability; tumor cells

GAP JUNCTION CHANNELS are formed by members of the connexin multigene family. At least a dozen connexin members have been identified from mammalian cells, with additional clones found in birds and amphibians. Western and Northern blot analyses of various tissues have indicated that connexin expression is tissue specific yet overlapping, and it is widely speculated that the existence of so many connexins is related to their specific sets of regulatory properties (11). Indeed, physiological studies have demonstrated differences in the gating properties of numerous individual connexins after expression in *Xenopus* oocytes (see Ref. 36 for review). However, it has become increasingly clear that properties of connexin channels as expressed in *Xenopus* oocytes may differ strikingly from those of the same connexins expressed either endogenously or exogenously in mammalian cells (for example, compare Ref. 3 with Refs. 27, 29; and compare Ref. 2 with Ref. 32). From the standpoint of understanding the properties of the individual mammalian connexins, it has thus become imperative to characterize the properties of the individual mammalian connexin channels both after exogenous expression in mammalian cell lines and in cell types in which the corresponding connexin uniquely composes the channels.

The SKHep1 cell line exhibits a very low degree of electrical coupling and has therefore been useful as a communication-deficient parental population in which exogenous expression can be seen against a very low endogenous background (13–15, 27–34, 40). However, some pairs of these cells obtained from the American Type Culture Collection do express a population of endogenous gap junction channels, which are characterized by very low unitary conductances (~30 pS; Ref. 28). To exclude their contribution to the behavior of the transfectants, it has been desirable to characterize the properties of the channels expressed in the parental line. In addition, the unique unitary conductance of the endogenous channels suggested that they might represent the endogenous expression of a connexin not previously examined electrophysiologically.

To obtain cells in which the expression of this channel type was more readily seen, we have established subclones of the parental line through isolation of colonies after plating the cells at low density. Several of the subclones displaying markedly different morphologies were then examined electrophysiologically, and one of these was found to exhibit a single population of channels with unitary conductances similar to those encountered in our previous studies of the parental line. With this clone, where macroscopic conductance and incidence of coupling were higher than in the parental cell line, we have assayed the type of connexin expressed and the biophysical properties of the channels including their open probabilities (P_o) at various voltages.

METHODS

Cells. The studies reported in this paper were performed on SKHep1 cells, either a population of cells received in 1989 from American Type Culture Collection or clones of cells repeatedly passaged from 1989 to 1992 then subcloned by dilution (M. Urban, D. C. Spray, and A. P. Moreno, unpublished data). The clone selected for these studies was designated SKHep1A and resembled morphologically the original SKHep1 cell line.

RNA blots. Total cellular RNA was prepared from SKHep1A cells or tissues (9), separated on formaldehyde agarose gels, and transferred to nylon membranes as previously described (7). Integrity of RNA samples was verified by ethidium bromide staining of gels or hybridization with 18S mRNA probes. Hybridization was performed using specific ^{32}P-labeled DNA probes (sp act $\approx 10^9$ counts·min^{-1}·μg^{-1}) prepared using ran-

dom hexanucleotide primers and the Klenow fragment of DNA polymerase I (5). Specific probes for human connexin (Cx) 40, Cx43, and Cx45 were prepared as described previously (7, 20, 22). The human Cx45 and Cx40 sequences, which are closely homologous to those previously cloned from other species, were amplified from human genomic DNA by the polymerase chain reaction (22) and have been submitted to GenBank (accession numbers U03846 and U03493).

Anticonnexin antibodies. Rabbit polyclonal antisera against Cx45 and Cx40 were raised as described previously using synthetic peptides representing amino acids 285–298 of dog Cx45 or 316–329 of dog Cx40 conjugated to keyhole limpet hemocyanin via a cysteine residue added to the NH_2-terminal end (21). The anti-Cx45 and anti-Cx40 antibodies were affinity purified by chromatography (Sulfolink coupling gel, Pierce Chemical, Rockford, IL) on agarose derivatized with this peptide according to the manufacturer's instructions and eluted with 0.1 M glycine, pH 3. A rabbit antiserum directed against a synthetic peptide representing amino acids 252–271 in Cx43 was produced previously and has been extensively characterized (6); this antiserum was used as a control reagent in some experiments. All three anticonnexin antisera have been demonstrated to react with gap junctions structures by electron microscopic immunocytochemistry (21). The specificity of these reagents has been demonstrated by immunoprecipitation of the corresponding polypeptides translated in vitro from the cloned DNAs (20).

Immunofluorescence. Cells adherent to glass microscope slides (Nunc, Naperville, IL) were fixed in a 50% methanol-50% acetone for 2 min at room temperature and permeabilized in 1% Triton X-100 phosphate-buffered saline (PBS). The permeabilized cells were then incubated in primary antibody (affinity-purified rabbit polyclonal anti-Cx45, 1:500 dilution) and secondary antibody (fluorescein-conjugated goat anti-rabbit immunoglobulin G, 1:1,000 dilution) at room temperature with intervening washes. The coverslips were viewed on a Nikon epifluorescence microscope with the appropriate barrier filters. Secondary antibody reagents were obtained from Boehringer Mannheim (Indianapolis, IN).

Immunoprecipitation. Cells were labeled for 2 h in the presence of methionine-depleted Dulbecco's modified Eagle's medium containing [^{35}S]methionine (100 μCi/ml) at 37°C. Labeled cells were harvested by scraping and were then lysed by sonication (4 × 15 s). Cell debris was concentrated by centrifugation (10 min, 14,000 *g*). The residue was then boiled in RIPA buffer {PBS with 1% Triton X-100, 1% 3-[(3-cholamidopropyl)dimethylammonio]-1-propanesulfonate, and 0.6% sodium dodecyl sulfate (SDS)} and 0.1 mg/ml aprotinin, 100 mM NaF, and 200 mM EDTA for 5 min. Cellular debris was collected by centrifugation (14,000 *g*, 15 min), and the supernatant was added to tubes containing 10 μl anti-Cx43 antisera, 1 μg anti-Cx45 or anti-Cx40 antibody, or 10 μl anti-Cx43 antiserum and 20 μl rProtein A-IPA 300 (Repligen, Cambridge, MA). These tubes were incubated with shaking at 4°C for 2 h. The pellets were collected with brief centrifugation. These tubes were washed four times in RIPA buffer, then analyzed by SDS-polyacrylamide gel electrophoresis on a 12.5% gel and subjected to fluorography.

Electrophysiological characterization of macroscopic junctional conductance. Junctional conductance (g_j) was measured between cell pairs using the dual whole cell voltage-clamp technique (35, 44). Access to the cytoplasm was achieved using a brief negative-pressure pulse after gigaohm seal formation between polished glass micropipettes (3–5 MΩ) and the cell membrane. To increase input resistance and to provide cells with ATP, the micropipettes were filled with cesium- and ATP-containing patch solution [in mM: 130 CsCl, 0.5 $CaCl_2$, 2 Na_2ATP, 3 MgATP, 10 *N*-2-hydroxyethylpiperazine-*N*′-2-ethanesulfonic acid (HEPES), and 10 ethylene glycol-bis(β-aminoethyl ether)-*N*,*N*,*N*′,*N*′-tetraacetic acid, pH 7.2]. During recording, cells were kept at room temperature and in cesium-containing bathing solution (in mM: 160 NaCl, 7 CsCl, 0.1 $CaCl_2$, 0.6 $MgCl_2$, and 10 HEPES, pH 7.4). To determine the voltage sensitivity of junctional channels, transjunctional current (I_j) was measured in one of the cells (held at constant voltage) while a protocol of voltage steps (ranging from −80 to 80 mV, increasing by 10 or 20 mV) was applied to the contiguous cell (using pCLAMP software; Axon Instruments). Best fits for current inactivation were obtained using clampfit (pCLAMP), and measurement of digitized records was done using pCLAMP's Clampex software. All current traces were digitized (Neurodata) and stored on a videocassette recorder tape. Parameters of voltage dependence were determined by normalizing the steady-state current (I_{ss}) levels during long voltage pulses with regard to the instantaneous current (I_{inst}) measured at the beginning of the pulses; normalized conductances are designated by *G*. The steady-state conductance (g_{ss}) values were fitted using pCLAMP software to the Boltzmann equation

$$g_j = \frac{g_{inst} - g_{ss}}{1 + \exp[A(V - V_0)]} + g_{min} \quad (1)$$

where g_j is macroscopic junctional conductance; g_{inst} and g_{ss} are instantaneous and steady-state conductance, respectively; *A* is steepness of relation; *V* is voltage; and V_0 is voltage at which voltage-sensitive conductance is reduced by 50%.

Single-channel analysis. Measurement of single-channel currents was achieved either by using freshly split cells where junctional conductance was low or reducing the total conductance by superfusing the cells with external solution containing halothane (2 mM). Open-time measurements were done using only low-conductance cell pairs (no halothane was required). Unitary junctional currents were obtained during long voltage steps applied to one of the cells. The unitary opening or closing current events were measured using a digitizing board (Summagraphics with SigmaScan software; Jandel, Corta Madera CA). Probability distribution histograms of the events (Sigmaplot; Jandel) and Gaussian distribution best fits were calculated for each experiment (Peakfit; Jandel). P_o values for each voltage step were determined by adding the time (during steady-state conditions) that the current spent at each conductance level (current trace filtered at 100 Hz) and dividing by the total steady-state duration and the total number of conductive levels. P_o values for each level were predicted by a binomial equation (see below) with the assumptions that *1*) the channels gated independently, *2*) they all had the same unitary conductance, and *3*) number of conductive levels and the unitary conductance were known. For multichannel preparations, according to Ref. 10

$$P_k = \frac{n!}{k! \times (n - k)!} \times P_o^k \times (1 - P_o)^{(n-k)} \quad (2)$$

where P_k is the probability of occurrence of any state *k*, *n* is the number of conductive levels, and P_o is obtained as the best fit of the P_k distribution. To optimize the fitting, $n + 1$, $n + 2$, and $n - 1$ channels were also tested in the equation.

Kinetic rate constants. Because the time course of junctional current inactivation was well described at each voltage by a monoexponential function, these junctional channels behaved as if the process of opening and closing of each hemichannel is governed by a simple two-state model with two voltage-dependent rate constants. As previously applied to amphibian gap junctions (17), the voltage-dependent rate constants for

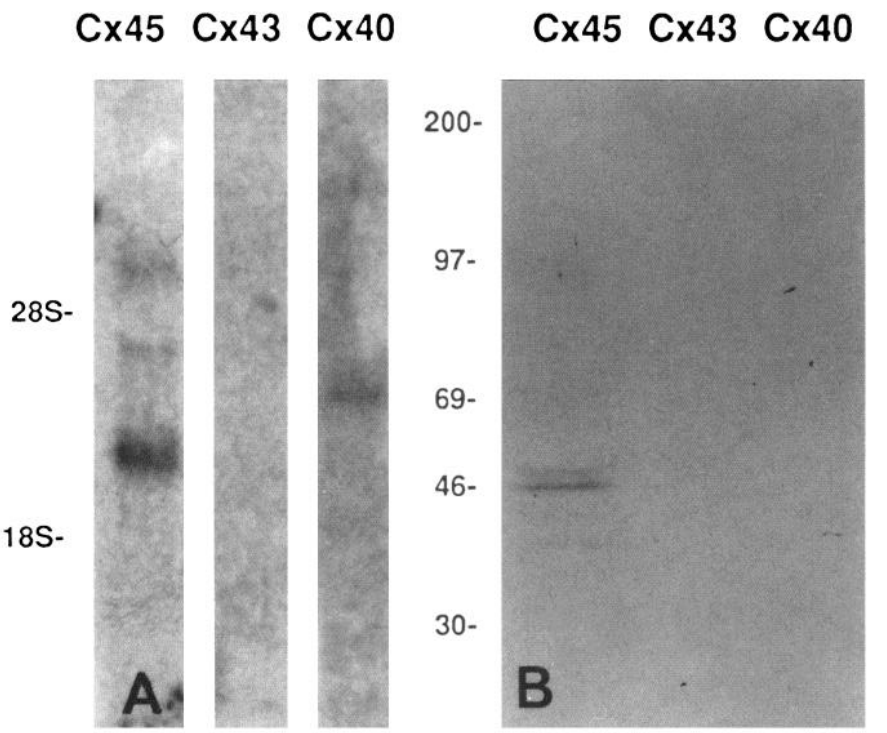

Fig. 1. Expression of connexin mRNAs and proteins by SKHep1A cells. *A*: Northern blot. Total cellular RNA was prepared from SKHep1A cells. RNA (10 μg) was resolved on a 1% agarose-formaldehyde gel, transferred to a nylon membrane, and hybridized with specific probes for human connexin (Cx) 45, Cx43, or Cx40 as indicated. Blots for Cx45 were exposed 2 days. Those from Cx40 and Cx43 were exposed for 7 days. *B*: immunoprecipitation of connexin proteins. SKHep1A cells were metabolically labeled with [^{35}S]methionine, and lysates were immunoprecipitated with anti-Cx40, anti-Cx43, or anti-Cx45 antibodies as outlined in METHODS. Immunoprecipitated materials were analyzed on a 12.5% polyacrylamide gel and subjected to fluorography. Protein molecular mass standards are indicated on *left*.

opening (α) and closing (β) were calculated from g_{ss} ($= I_{ss}/V_j$) and the time constant (τ) for each voltage [$\alpha = G_{ss}/\tau$; $\beta = (1 - G_{ss})/\tau$]. The parameters that govern α and β were calculated from these rate constants and fitted to the equations: $\alpha = \lambda[-A_\alpha(V - V_0)]$; $\beta = \lambda[A_\beta(V - V_0)]$, where α and β are the opening and closing rate constants, respectively; λ is the rate constant where $\alpha = \beta$ at V_0; and A_α and A_β are the voltage sensitivities of the opening and closing rate constants, respectively.

RESULTS

Gap junctions in SKHep1A are formed of Cx45. To determine which connexin was expressed by the SKHep1A cells, we initially screened these cells for expression of connexin mRNAs by Northern blotting. We detected no significant hybridization of SKHep1A RNA with ^{32}P-labeled probes for Cx26, Cx31, Cx32, Cx37, Cx38, Cx42, Cx43, Cx46, or Cx50. However, we observed strong hybridization of probes corresponding to canine or human Cx45 to a band of ≈2.2 kDa in the SKHep1A RNA (Fig. 1*A*). Cx45 mRNAs of similar mobility have previously been found in studies of other cells (18, 21). In addition, as previously reported for the parental SKHep1 cell line (4), weak hybridization was obtained using a probe specific for Cx40. Comparing the

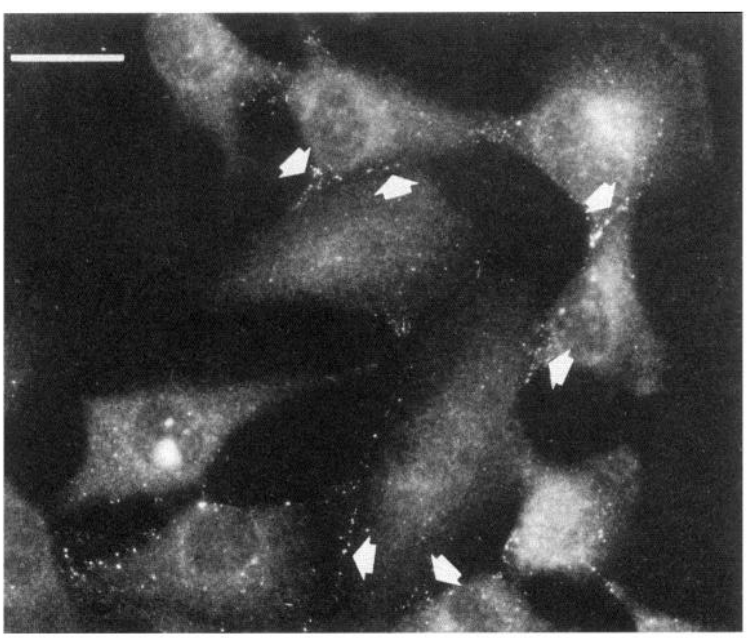

Fig. 2. Immunofluorescence analysis of Cx45 in SKHep1 cells. Cultured SKHep1 cells were fixed and permeabilized with Triton X-100, then stained with rabbit anti-Cx45 antibodies followed by a fluorescent secondary reagent. Cx45 reactivity localized to bright spots, many of which were at appositional surfaces between cells as indicated by arrows. Bar, 15 μm.

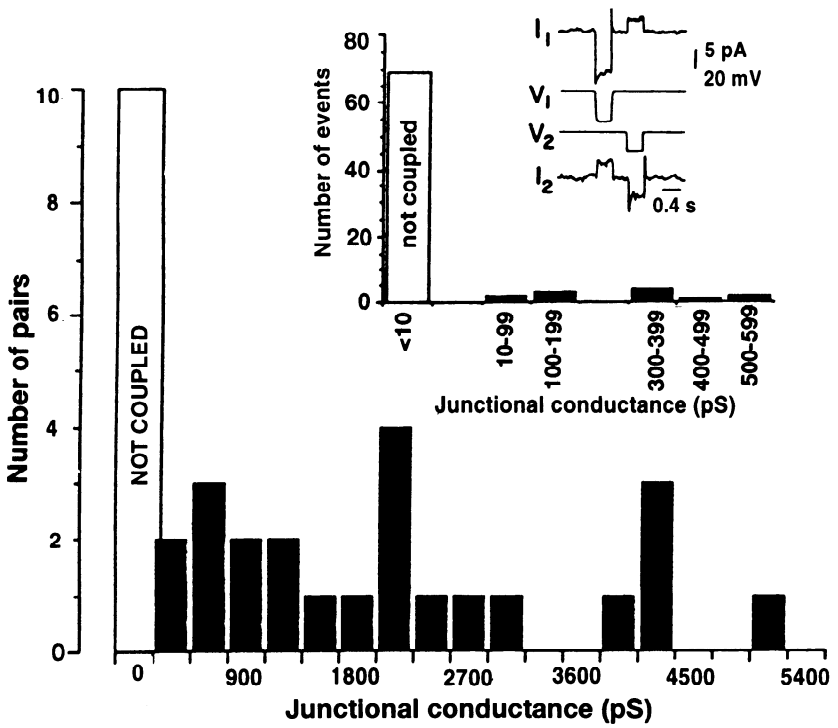

Fig. 3. Macroscopic junction conductances recorded between SKHep1 cell pairs in this study. *Inset*: junctional conductance measured in 81 pairs in a previous study, where most pairs were totally uncoupled (27). *I*, current; *V*, voltage. Major portion of figure shows distribution of junctional conductance values recorded from SKHep1A. In these 33 cell pairs, macroscopic junctional conductance ranged from <10 pS (lower resolution limit, 30% of pairs) to 5 nS. Mean junctional conductance for all cells tried was 1.36 ± 1.46 nS.

relative intensities of the bands and the threefold longer exposure time of the Cx45 blot suggests that Cx45 mRNA was much more abundant than Cx40 mRNA in these cells.

Immunofluorescence and immunoprecipitation were two strategies used to confirm that these cells indeed expressed the Cx45 protein. Immunoprecipitation of [^{35}S]methionine-labeled SKHep1A lysates with anti-Cx45 antibodies yielded a single major band of ≈48 kDa (Fig. 1*B*). This band had a mobility similar to that which we have observed in a number of other Cx45-expressing cell lines (23). In contrast, nonimmune reagents or antibodies to Cx40 or Cx43 (Fig. 1*B*) gave no specific precipitation from these cells. The Cx45 mRNA and protein were also demonstrated (although at lower levels) in the parental SKHep1 cells (data not shown). Immunofluorescent staining of the SKHep1A cells with anti-Cx45 antibodies produced a pattern of bright spots at the appositional surfaces between adjacent cells consistent with that typically seen for gap junctions (Fig. 2). Anti-Cx40 or anti-Cx43 antibodies showed no reactivity with these cells (data not shown).

Macroscopic and microscopic conductance of channels formed by Cx45. We previously reported that the unitary conductance of the endogenous channels in SKHep1 cells was 29 ± 6 pS (28). The connexin corresponding to these small-conductance channels appears to be Cx45 as summarized above. The original report dealing with these cells indicated the presence of few channels between them, as the g_j was in all cases <600 pS (Fig. 3, *inset*). The subclone chosen for the present studies (SKHep1A) showed a single population of channels and exhibited low g_j, although g_j was somewhat higher than that previously found for the parental population (range between 0.01 and 5 nS; mean g_j between all coupled cell pairs was 1.3 nS, Fig. 3).

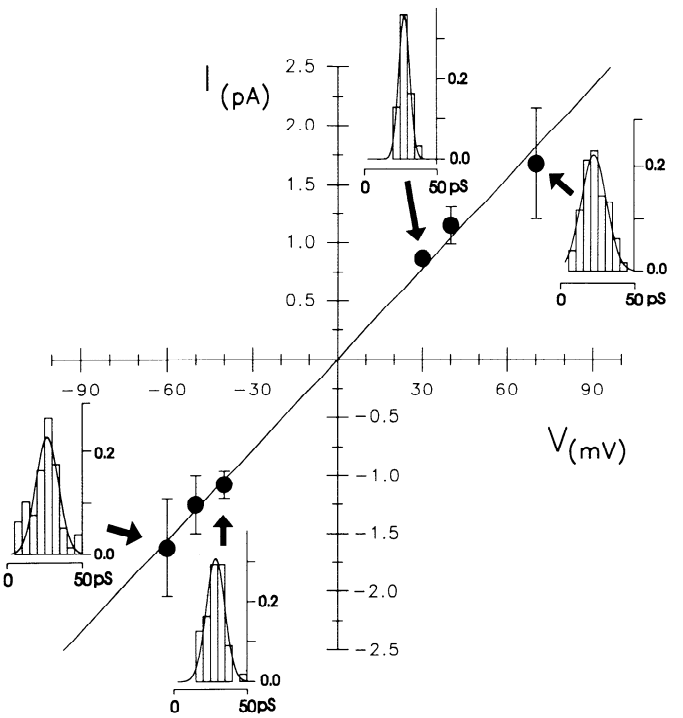

Fig. 4. Unitary conductance of human Cx45 gap junction channels measured at various transmembrane voltages. Current (*I*)-voltage (*V*) curve shown was obtained from unitary junctional currents measured at different voltages in a preparation in which 4 channels were present in junction. More than 100 events were measured at each voltage. Events at high voltages were obtained through a reverse potential protocol (see Fig. 7). Each frequency histogram shows Gaussian distributions corresponding to points indicated. *X*-axis represents unitary conductance in 5-pS bins; *y*-axis is frequency of events recorded. For pulses shown (−60, −40, 30, and 70 mV), means ± SD of best-fit Gaussian distributions are 28 ± 7, 28 ± 4, 29 ± 6, and 24 ± 8 pS, respectively, with r^2 values of 0.89, 0.99, 0.97, and 0.96, respectively. Best linear fit to all points in *I-V* relation yields a slope of 27 ± 3 pS. Note from histograms that at highest transjunctional voltage values there are numerous events at lower conductance levels.

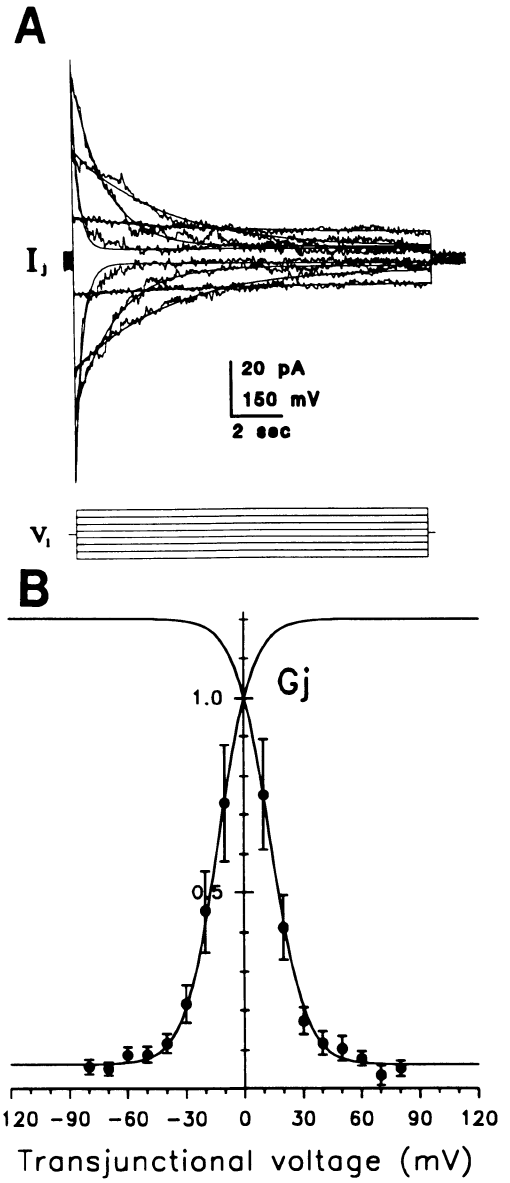

Fig. 5. Macroscopic voltage dependence of gap junction channels in SKHep1 cells. *A*: digitized traces of junctional current (I_j) relaxation during a protocol of pulses (*bottom*) applied to 1 cell of a pair. Superimposed on each data trace is best fit of relaxation to a single exponential function, from which time constant data were obtained (Fig. 6). I_j at end of pulses, divided by transjunctional voltage, gave steady-state junctional conductance (g_{ss}) values. *B*: voltage dependence of g_{ss}. Data from 7 experiments with average junctional conductance values (G_j) of 3.01 ± 1.24 nS were used. Boltzmann relation (see METHODS) was fit to averaged data with the following parameters: V_0 = 13.4 mV, A = 0.115, G_{max} = 1.20, and g_{min}/g_{max} = 0.061.

The unitary conductances of the junctional channels were determined from histograms constructed from experiments in which >100 event amplitudes were measured at different voltages (Fig. 4). For each histogram, peak amplitude was obtained as the best fit of the data to a Gaussian distribution. Values of I_j plotted in Fig. 4 are means ± SD of these Gaussian fits. Over a wide range of voltages (−60 to +70 mV), the mean unitary conductance of these channels was constant (Fig. 4), with a slope conductance of 27 ± 3 pS, as determined by linear regression. Note that smaller events are detected at the highest voltages (especially clear in histogram corresponding to −60 mV, Fig. 4). The average value of unitary conductance for five different cell pairs at 30–50 mV was 28 ± 6 pS.

Macroscopic voltage-dependent characteristics. During application of a family of voltage pulses (V_j, Fig. 5*A*), I_j relaxed monoexponentially to reach steady-state values at the end of each pulse (curve fits superimposing data in Fig. 5*A*). This I_{ss} value was normalized with respect to the initial current at the beginning of each

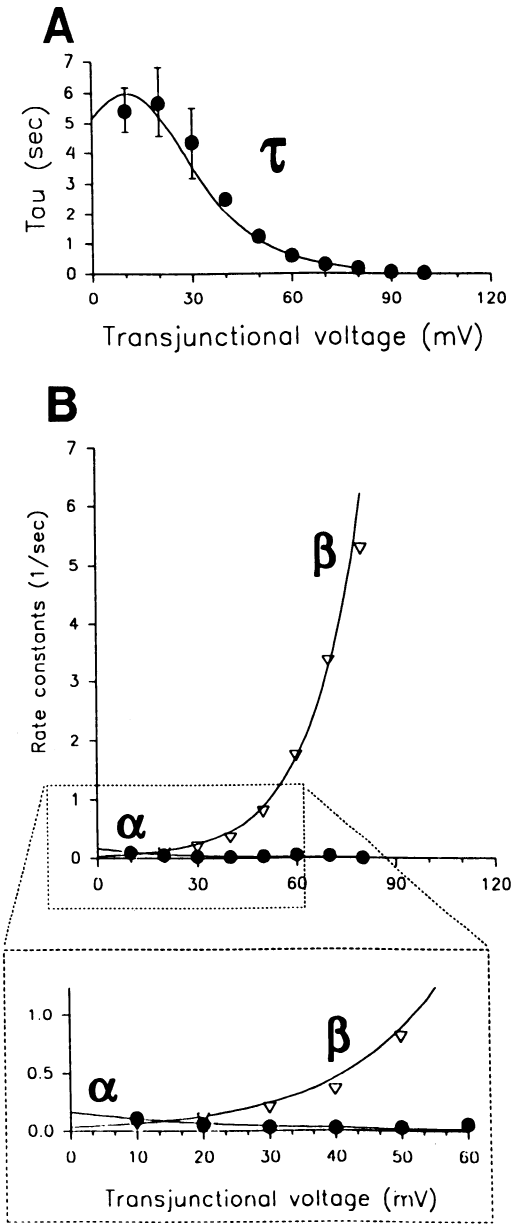

Fig. 6. Opening and closing time and rate constants for human Cx45 gap junction channels are quite voltage dependent. *A*: time constants (τ) for each V_j pulses from 10 to 100 mV in 10-mV increments were averaged from 6 experiments for both positive and negative V_j values. *B*: opening rate constant (α) and closing rate constant (β) were calculated for each voltage from time constant data in *A* and g_{ss} data presented in Fig. 5*B*, using equations presented in METHODS. Note that β does not saturate at highest voltages, and, as seen in magnified portion of record, α and β are weakly voltage dependent at low V_j.

voltage pulse to obtain G_{ss}, which was plotted as a function of V_j as shown in Fig. 5*B*. The best fit for a Boltzmann relation using the average of seven different experiments (where only 30-pS channels were detected after exposure of cells to halothane) is shown as a continuous line superimposed on the averaged data. The parameters for the best fit of the Boltzmann relation to the data set are as follows: V_0, 13.4 mV; A, 0.115; G_{max}, 1.202; and G_{min}/G_{max}, 0.06. Note that each of the symmetric Boltzmann relations intersects the ordinate at G_{ss} values lower than G_{max}. Consistent with other nomenclature introduced elsewhere (8), we designate G_{ss} at 0 mV to equal 1.0; G_{max} obtained from the best fit to the Boltzmann equation is thus 1.2, indicating that 20% of the junctional channels are closed at transjunctional voltage of 0 mV.

Kinetic constants. The process of relaxation of junctional conductance in response to voltage pulses could be adequately described with monoexponential functions even at very high voltages (±100 mV; Fig. 5*A*). Time constants for relaxation were larger (≈ 6 s) for transjunctional voltage steps near V_0 and declined to ~200 ms at voltages higher than ±80 mV (Fig. 6*A*). As was described previously (17, 29), the rate constants α and β (for opening and closing) for a two-state model should describe accurately the velocity of change between the two states; α and β (see above) are also voltage dependent and for values up to ±70 mV, each rate constant follows the equations with parameters of λ, 0.35 s^{-1}; A_α, 0.45 mV^{-1}; A_β, 0.65 mV^{-1}; and V_0, 14 mV. These parameters demonstrate that the closing rate constant is ≈ 1.5 times more sensitive to voltage than the opening rate constants over the entire voltage range (Fig. 6*B*).

Contingent gating. Because gap junction channels are believed to be formed by two hemichannels connected head to head, and because closures are achieved by either polarity of voltage applied to either side of the junction, a model of two gates per channel was originally proposed in which each gate was responsible for closure of one hemichannel by voltage of one polarity (39). The contingent gating model requires that, when polarity of the voltage is reversed, the gate closed by the prepulse must open before the gate in series with it senses the transjunctional voltage and can subsequently close (17). To test whether this model was applicable to the behavior of Cx45 gap junction channels, a polarity reversal protocol was applied. The data presented in Fig. 7 support the conclusion that the channels must indeed first open before they can close. However, in contrast to the behavior of channels formed by *Xenopus* Cx38 (17) and rat Cx32 (29), the peak current I_j observed during the test pulse was substantially delayed and diminished compared with behavior expected. A factor that could account for this difference is that G_{max} is 1.2, indicating that some junctional channels are closed at V_j of zero (Fig. 5*B*). To model this behavior, it will be necessary to consider a new term (β_1, see Ref. 17) in the equation that predicts the responses to currents during the test pulse.

Aspects of Cx45 voltage dependence revealed in single-channel recordings. The extraordinarily low expression of functional gap junction channels encountered between SKHep1 cell pairs has allowed us to determine the P_o of Cx45 channels over a range of transjunctional voltage in the absence of halothane treatment. Experiments in which the maximal junctional conductance at low V_j values indicated the presence of two and five total

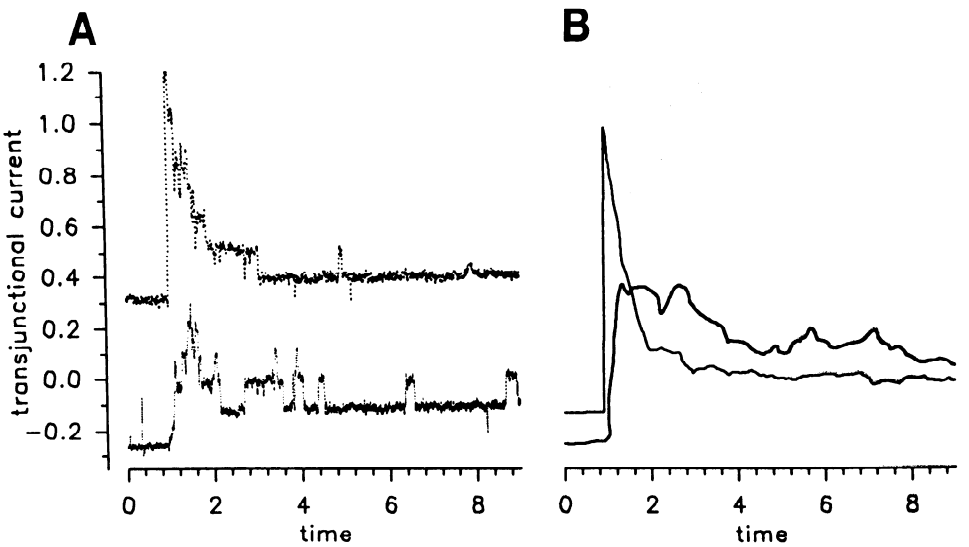

Fig. 7. Evidence for contingent gating in human Cx45 gap junction channels. *A*: 2 traces in which channel number was low, showing behavior of unitary currents during relaxation of junctional current during a 70-mV pulse. *Top trace* corresponds to a control pulse in which 5 conductance levels were clearly seen, and its baseline was moved upward 0.3 units for clarity. Instantaneous maximal current (upward deflection) decreased over a time course of ~2 s to lowest conductance level. *Bottom trace* corresponds to a pulse of similar magnitude but applied immediately after a pulse of opposite polarity has been applied for 10 s so that a steady-state level of decreased macroscopic conductance was previously reached. Maximal conductance is attained with a delay compared with faint trace, and continued channel activity extends for several seconds thereafter. Thus channels first opened before closing. *B*: control and test currents as shown in *A*, but at a macroscopic level. All traces were normalized to instantaneous macroscopic current shown in *B*, during control voltage pulse.

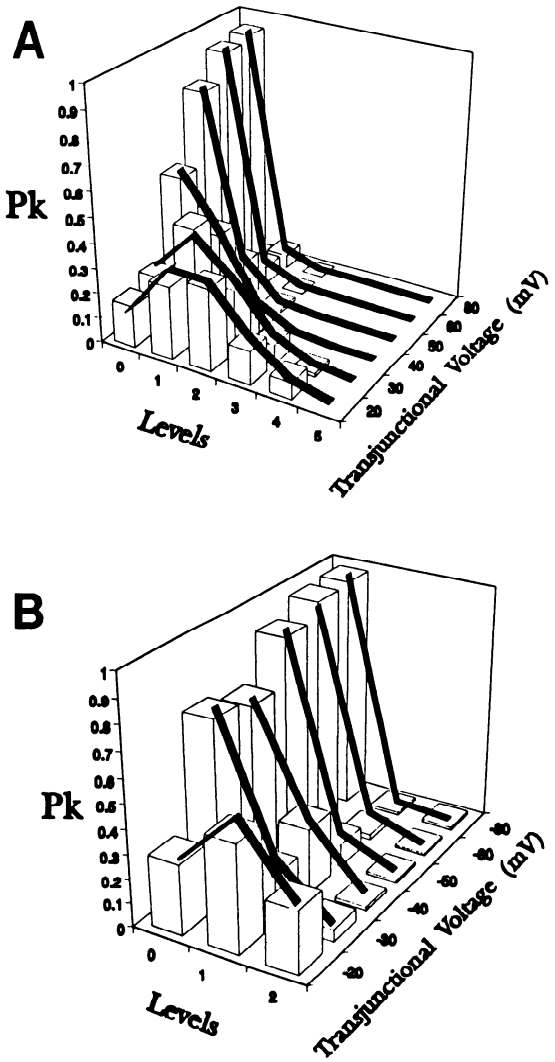

Fig. 8. Microscopic open probability (P_o) for human Cx45 channels matches values predicted by a binomial distribution with values obtained from macroscopic parameters of voltage dependence. P_k, probability of occurrence of any state k. Two experiments were selected for this analysis in which total number of channels was 5 (*A*) and 2 (*B*). Values of P_o for each voltage (see METHODS) were measured after steady state was reached ($\sim 2\ \tau$ values); these are shown as columns, together with best fit values (thick lines) obtained according to *Eq. 2* in METHODS.

channels connecting the cell pairs are shown in Fig. 8, *A* and *B*. Some of the original recordings are illustrated in Fig. 10. The sampling times used were 24, 34, 45, 39, 37, and 12 s for Fig. 8*A* and 18, 17, 37, 25, 36, and 18 s for Fig. 8*B*; in both experiments, they correspond to ±80, 60, 50, 40, 30, and 20 mV, respectively. The percentage of time spent at each conductance level was measured after steady state was reached. Probabilities of channels being in each conductance state (0 open to n open) were calculated as indicated in METHODS and were plotted together with the predicted behavior based on voltage dependence of G_j determined from macroscopic recordings. Other recordings and best fits (not shown) demonstrated that a maximum of five channels were present between these cells. P_o values obtained for these experiments are plotted as a function of V_j in Fig. 9, with G_j offset by 0.05 to account for g_{min}. It is clear from this plot and from records like those in Fig. 10 that P_o for these channels approaches zero at $V_j > 50$ mV and, therefore, that G_{min} is not attributable to the continued openings of these channels at high voltages.

The observed match between voltage dependence of P_o and of macroscopic g_j indicates that the macroscopic contingency gating experiments should have as microscopic counterparts the opening of channels before they close. Such behavior, from a cell pair with five initially open channels, is illustrated in Fig. 7. At the beginning of the control pulse to 70 mV, all channels close within ~ 2 s in 30-pS decrements, leaving a small residual g_j (analogous to g_{min} observed in macroscopic data) (Fig. 7, dotted line). When this pulse was preceded by an equal-sized pulse of opposite polarity, the channels first traveled through a period of maximal activity (3 channels open, occurring 0.5 s after reversal of the pulse), followed by opening then closing. Steady-state channel activity was reached at ~ 4.5 s after the reversal (Fig. 7, dashed line). This difference in time course is consistent with the delay seen in peak I_j in macroscopic polarity reversal experiments (Fig. 7*B*).

DISCUSSION

We report in this study that a subclone of SKHep1 exhibited Cx45 gap junction mRNA and protein as evidenced by immunoprecipitation and immunocytochemical staining of the cells in culture. These cells also express very low levels of Cx40 mRNA (as found for the parental SKHep1 cells; Ref. 4) but no detectable Cx40 protein. No expression of mRNA corresponding to any

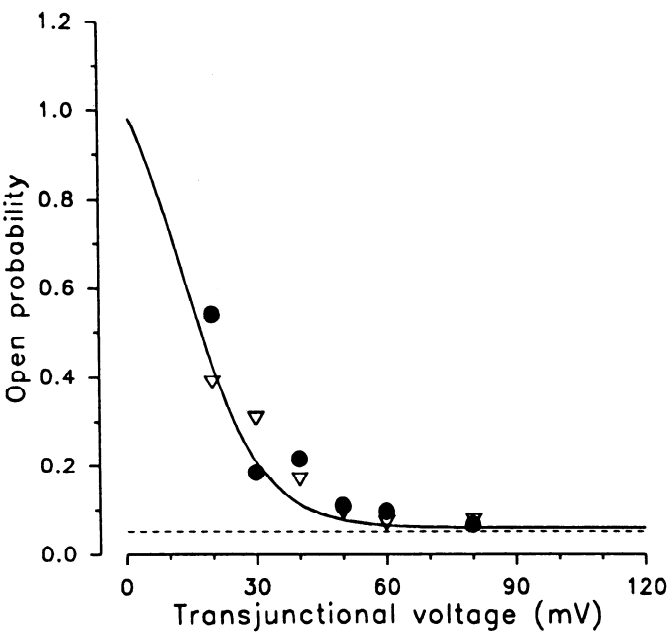

Fig. 9. Microscopic voltage-dependent P_o matches macroscopic voltage dependence. Best fit values for P_o obtained for experiments where 2 (●) and 5 channels (▽) were present between SKHep1 cells, can be superimposed to best fit of Boltzmann equation for macroscopic voltage dependence shown in Fig. 5*B* (solid line). Dashed line represents normalized minimum conductance.

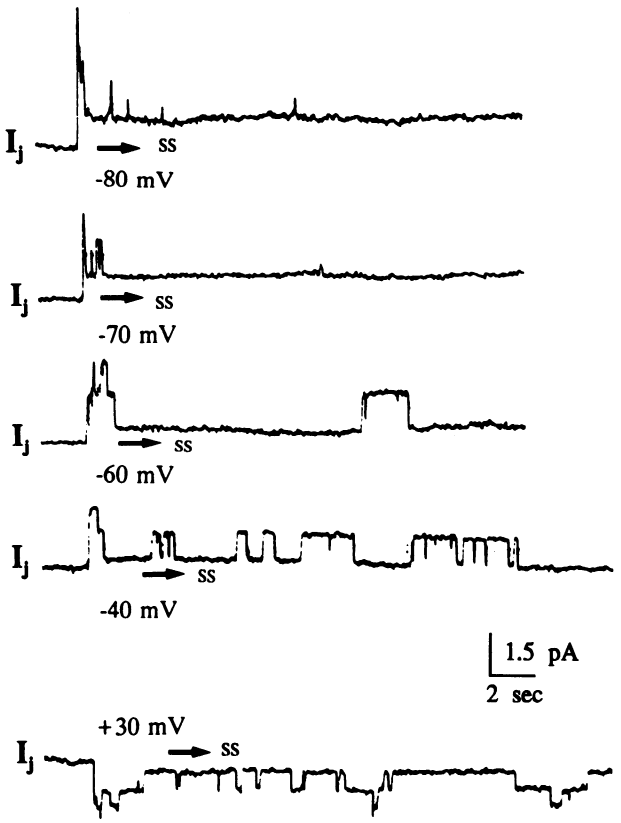

Fig. 10. Voltage dependence of human Cx45 channels at microscopic level. All junctional traces were recorded from same cell pair during transjunctional pulses of −80, −70, −60, −40, and +30 mV. Notice that open times of larger conductance level were reduced as transjunctional voltage increased. Arrows labeled SS represent onset of steady-state level as determined from relaxation of macroscopic current in other experiments (see Fig. 6), as well as zero junctional conductance levels. I_j, junctional current.

other identified connexin was found. We conclude that the gap junction channels present in these SKHep1A cells are composed of Cx45. It should be noted that other subclones of our passaged cell line exhibit gap junction channels with different properties (M. Urban, D. C. Spray, and A. P. Moreno, unpublished data), and this diversity in subclones raises the caution that early passages of well-characterized cells should be maintained for transfection experiments. Indeed, preliminary observations suggest that one such clone shows significant functional expression of Cx40.

Our electrophysiological characterization of human Cx45 channels indicates that their unitary conductances (γ_j) are quite small, on the order of 30 pS, and that the gating is highly sensitive to transjunctional voltage with V_0 equal to 13.4 mV and A equal to 0.115. Studies using chick Cx45 (which is 92% similar to the human Cx45 at the amino acid level) expressed in another communication-deficient mammalian cell line (N2A rat neuroblastoma cells) indicated that chick Cx45 channels also displayed γ_j values of ~30 pS (43). The voltage dependence of the chick Cx45 channels, however, was strikingly less than that observed in our studies on human Cx45 (Table 1). With the assumption that this difference is not ascribable to differences in access resistance in their experiments (see Refs. 29, 45), the examination of sequence differences may provide clues to the structure of the voltage sensor, which has remained elusive in the extensive domain substitution analyses of rat Cx32 and rat Cx26 (37).

The voltage sensitivity that we report here for human Cx45 channels is much steeper than previously reported for any other mammalian connexin (parameters summarized in Table 1) and is even somewhat steeper than for the 40-pS gap junction channels recently reported between rat Schwann cells (8). These findings indicate that in heart, and presumably elsewhere in higher mammals, gap junction channels exist with exquisite voltage sensitivity, as high as reported previously in *Xenopus* Cx38, either endogenously expressed in the early amphibian embryo (17, 38, 39) or after exogenous expression in SKHep1 cells (31) or in *Xenopus* oocytes (12).

Although the equivalent gating charge appears markedly conserved among the mammalian connexin channels examined to date in mammalian cells (ranging from 1.7 to 2.9, see Table 1), V_0 ranges from ~14 mV for human Cx45 to 60 mV for human Cx43. The low V_0 in Cx45 and in rat Schwann cells indicates that g_j will be highly sensitive to small differences in resting potentials in cells coupled through these channels. As was presented previously (17), the energy difference between the open state of the channel and the state closed by voltage is proportional to AV_0. For the connexins listed in Table 1, these values are 1.55 kcal/mol (human Cx45), 2.15 kcal/mol (chick Cx45), 3.5 kcal/mol (*Xenopus* Cx38), 1.75 kcal/mol (rat Cx32), 6.36 kcal/mol

Table 1. *Parameters of voltage dependence of connexins in mammalian cells*

	hCx45	cCx45	XCx38	rCx32	hCx43	Schwann
V_0, mV	13.5	39	14	27	60	17
A (n)	0.115 (2.9)	0.055 (1.4)	0.25 (6.25)	0.065 (1.7)	0.106 (2.7)	0.096 (2.4)
g_{min}/g_{max}	0.06	0.09	0.05	0.1	0.37	0.1
A_α, mV^{-1}	0.045	NA	0.077	0.023	0.008	0.002
A_β, mV^{-1}	0.065	NA	0.14	0.034	0.057	0.076

Boltzmann equation parameters that best fit to behavior of macroscopic conductance of different types of connexins are shown. V_0, voltage at which voltage-sensitive conductance is reduced by 50%; A, steepness of relation (equivalent gating charge $n = AKT/q$ is given in parentheses); g_{min}/g_{max}, fraction of residual to total conductance; A_α and A_β, voltage sensitivities of opening and closing rates, respectively; NA, not analyzed. Data were obtained from the following sources: human connexin 45 (hCx45), present study; chick connexin 45 (cCx45), Ref. 43; *Xenopus* connexin 38 (XCx38), Ref. 31; rat connexin32 (rCx32), Ref. 29; human connexin 43 (hCx43), Ref. 32 and unpublished values for dephospho forms; rat Schwann cells, Ref. 8.

(human Cx43), and 1.63 kcal/mol (Schwann cell 40-pS channel). For all the connexins listed in Table 1, the closing rate constants (A_β in Table 1) are from <2 to >30 times faster than the opening rate constants (A_α). Because V_0 for Cx45 channels is so low, this results in very fast time constants (<100 ms) for current relaxation at high voltages (greater than ± 70 mV). This closure is still quite slow by comparison with rectifying synapses (e.g., Refs. 1, 16), and it is of dubious physiological relevance. Even in the heart, Cx45 channels would not be expected to close during the protracted ventricular action potentials unless coupling was so weak that substantial transjunctional voltages developed.

The steady-state electrophysiological properties of human Cx45 are quite similar to those of *Xenopus* Cx38, which might be anticipated to indicate a similarity in primary sequence. We have therefore compared these sequences (12, 22) for regions of amino acid and base pair homology using a sequence analysis software package from the Genetics computer group for VAX/NUS computers. This analysis revealed that the identity between these connexins was in fact quite low, less than that for human Cx45 compared with the least voltage-dependent gap junction protein human Cx43 (Cx38 35% identical to Cx45, whereas Cx43 is 38% identical to Cx45). Comparisons of this type indicate that, regardless of the primary sequence of the entire connexin, there must be unique connexin sequences that confer upon each gap junction channel protein its particular response to applied transjunctional voltages.

Although inactivation time constants of transjunctional current were fitted to single exponentials, some deviation can be seen from the original curves (see Fig. 6) which cannot be consistently better fitted with two or more exponentials. One possible explanation for this discrepancy is that as many as 20% of the channels are closed at V_0; thus, during a transjunctional pulse, the two components would correspond to the majority of the channels that close their gates (according to the contingency model), and the other would correspond to those channels that were initially closed at V_0 but must open to close again. Because of these small deviations from expectation, and the low percentage of channels in the closed state at 0 mV, we have not attempted to improve these fits by including this possibility in our calculations.

The possibility that the number of channels packed in the membrane could affect their gating properties was eliminated by studying cell pairs exhibiting a uniform channel population where g_j was low enough to perform an analysis of the open time (P_o) of human Cx45 channels. Portions of the traces used for this type of analysis are shown in Fig. 10. Such kinetic analysis, which has previously been achievable only in two systems in which the connexin types remain unknown (rat Schwann cells, Ref. 8; and excised patches from earthworm septate regions, Ref. 25), also allows assessment of whether the microscopic transitions between open and closed states result from changes in open time, closed time, or unitary conductance of the channels.

Unitary conductances in the 30-pS range have been reported previously in several systems (between rat Schwann cells where $\gamma_j \approx 40$ pS, Ref. 8; *Xenopus* Cx38 expressed in SKHep1 cells with $\gamma_j \approx 40$ pS, Ref. 31; Cx43 substates $\gamma_j \approx 25$ pS, Ref. 33; chick Cx45 where $\gamma_j \approx 30$ pS, Ref. 43). One question that arises from these γ_j measurements is whether the low-conductance channels are less permeable to molecules of high molecular weight or exhibit more ionic selectivity than those larger channels formed of Cx32 or Cx43. With the assumption that all gap junction channels share a basic three-dimensional structure as is evidenced by the conserved membrane topology (19, 26, 46), pore sizes corresponding to predictions from γ_j can be compared. If the pores are filled by solute as conductive as cytoplasm (100 $\Omega \cdot$ cm), and the pore diameter is uniform over a length of 17 nm (24), the pore of the Cx45 channel would be expected to be ~ 12 nm, one-half as large as that formed by Cx32 ($\gamma_j \approx 130$ pS, Ref. 28) and two-thirds as large as that of Cx43 (14). Consistent with these calculations, Cx45 channels appear to possess extremely low permeability for Lucifer yellow; no dye coupling has been detected either in any of the clones that express Cx45 or in strongly coupled heterologous pairings of these cells with those expressing Cx43 (chick Cx45, Refs. 41, 42; human Cx45 and human Cx45-human Cx43, Ref. 30).

NOTE ADDED IN PROOF

The unitary conductance for chick Cx45 has been reported similar to the one presented here (see R. D. Veenstra, H. Z. Wang, E. C. Beyer, and P. R. Brink. *Circ. Res.* 75: 483–490, 1994).

A. P. Moreno was a recipient of a Grant-in-Aid from the New York State Affiliate of the American Heart Association. D. C. Spray was a recipient of the Beatrice F. Parvin Grant-in-Aid Award from the New York Affiliate of the American Heart Association. E. C. Beyer is an Established Investigator of the American Heart Association. Additional support was derived from National Institutes of Health Grants NS-12543 (to D. C. Spray), HL-45466 (to E. C. Beyer), and EY-08368 (to E. C. Beyer) and from a postdoctoral fellowship from the Lucille P. Markey Foundation (to J. G. Laing).

Address for reprint requests: A. P. Moreno, Dept. of Biological Sciences, SUNY at Buffalo, 628 Cooke Hall, Buffalo, NY 14260.

Received 22 September 1993; accepted in final form 23 August 1994.

REFERENCES

1. **Auerbach, A. A., and M. V. L. Bennett.** A rectifying electrotonic synapse in the central nervous system of a vertebrate. *J. Gen. Physiol.* 53: 211–237, 1969.
2. **Barrio, L. C., A. Handler, and M. V. L. Bennett.** Inside-outside and transjunctional voltage dependence of rat connexin43 channels expressed in pairs of *Xenopus* oocytes (Abstract). *Biophys. J.* 64: A191, 1993.
3. **Barrio, L. C., T. Suchyna, T. Bargiello, X. Xu, R. Roginski, M. V. L. Bennett, and B. J. Nicholson.** Voltage dependence of homo- and hetero-typic Cx26 and Cx32 gap junctions expressed in *Xenopus* oocytes. *Proc. Natl. Acad. Sci. USA* 88: 8410–8414, 1991.
4. **Beyer, E., K. E. Reed, E. M. Westphale, H. L. Kanter, and D. M. Larson.** Molecular cloning and expression of rat connexin40, a gap junction protein expressed in vascular smooth muscle. *J. Membr. Biol.* 127: 69–76, 1992.
5. **Beyer, E. C.** Molecular cloning and developmental expression of two chick embryo gap junction proteins. *J. Biol. Chem.* 265: 14439–14443, 1990.

6. **Beyer, E. C., J. Kistler, D. L. Paul, and D. A. Goodenough.** Antisera directed against connexin43 peptides react with a 43-kDa protein localized to gap junctions in myocardium and other tissues. *J. Cell Biol.* 108: 595–605, 1989.
7. **Beyer, E. C., D. L. Paul, and D. A. Goodenough.** Connexin43: a protein from rat heart homologous to a gap junction protein from liver. *J. Cell Biol.* 105: 2621–2629, 1987.
8. **Chanson, M., K. Chandross, M. B. Rook, J. A. Kessler, and D. C. Spray.** Gating characteristics of a steeply voltage-dependent gap junction channel in rat Schwann cells. *J. Gen. Physiol.* 102: 925–946, 1993.
9. **Chomczynski, P., and N. Sacchi.** Single step method of RNA isolation by acid guanidinium thiocyanate-phenol-chloroform extraction. *Anal. Biochem.* 162: 156–159, 1987.
10. **Colquhoun, D., and A. G. Hawkes.** The principles of the stochastic interpretation of ion-channel mechanisms. In: *Single Channel Recording,* edited by B. Sakmann and E. Neher. New York: Plenum, 1983, p. 135–177.
11. **Dermietzel, R., T. K. Hwang, and D. C. Spray.** The gap junction family: structure, function and chemistry. *Anat. Embryol.* 182: 517–528, 1990.
12. **Ebihara, L., E. C. Beyer, K. I. Swenson, D. L. Paul, and D. A. Goodenough.** Cloning and expression of a *Xenopus* embryonic gap junction protein. *Science Wash. DC* 243: 1194–1195, 1989.
13. **Eghbali, B., J. A. Kessler, and D. C. Spray.** Expression of gap junction channels in communication-incompetent cells after stable transfection with cDNA encoding connexin32. *Proc. Natl. Acad. Sci. USA* 87: 1328–1331, 1990.
14. **Fishman, G. I., A. P. Moreno, D. C. Spray, and L. A. Leinwand.** Functional analysis of human cardiac gap junction channel mutants. *Proc. Natl. Acad. Sci. USA* 88: 3525–3529, 1991.
15. **Fishman, G. I., D. C. Spray, and L. A. Leinwand.** Molecular characterization and functional expression of the human cardiac gap junction channel. *J. Cell Biol.* 111: 589–598, 1990.
16. **Furshpan, E. J., and D. D. Potter.** Transmission at the giant motor synapses of the crayfish. *J. Physiol. Lond.* 145: 289–325, 1959.
17. **Harris, A. L., D. C. Spray, and M. V. Bennett.** Kinetic properties of a voltage-dependent junctional conductance. *J. Gen. Physiol.* 77: 95–117, 1981.
18. **Hennemann, H., H. J. Schwarz, and K. Willecke.** Characterization of gap junction genes expressed in F9 embryonic carcinoma cells: molecular cloning of mouse connexin31 and -45 cDNAs. *Eur. J. Cell Biol.* 57: 51–58, 1992.
19. **Hertzberg, E. L., R. M. Disher, A. A. Tiller, Y. Zhou, and R. G. Cook.** Topology of the M_r 27,000 liver gap junction protein. Cytoplasmic localization of amino- and carboxyl termini and a hydrophilic domain which is protease-hypersensitive. *J. Biol. Chem.* 263: 19105–19111, 1988.
20. **Kanter, H. L., J. G. Laing, E. C. Beyer, K. J. Green, and J. E. Saffitz.** Multiple connexins co-localize in canine cardiac myocyte gap junctions. *Circ. Res.* 73: 344–350, 1993.
21. **Kanter, H. L., J. E. Saffitz, and E. C. Beyer.** Cardiac myocytes express multiple gap junction proteins. *Circ. Res.* 70: 438–444, 1992.
22. **Kanter, H. L., J. E. Saffitz, and E. C. Beyer.** Molecular cloning of two human gap junction proteins, connexin40 and connexin45. *J. Mol. Cell Cardiol.* 26: 861–868, 1994.
23. **Laing, J. G., E. M. Westphale, G. L. Engelmann, and E. C. Beyer.** Characterization of the gap junction protein connexin45. *J. Membr. Biol.* 139: 31–40, 1994.
24. **Makowski, L., D. L. Caspar, W. C. Phillips, and D. A. Goodenough.** Gap junction structures. V. Structural chemistry inferred from X-ray diffraction measurements on sucrose accessibility and trypsin susceptibility. *J. Mol. Biol.* 174: 449–481, 1984.
25. **Manivannan, K., S. V. Ramanan, R. T. Mathias, and P. R. Brink.** Multichannel recordings from membranes which contain gap junctions. *Biophys. J.* 61: 216–227, 1992.
26. **Milks, L. C., N. M. Kumar, R. Houghten, N. Unwin, and N. B. Gilula.** Topology of the 32-kDa liver gap junction protein determined by site-directed antibody localizations. *EMBO J.* 7: 2967–2975, 1988.
27. **Moreno, A. P., A. C. de Carvalho, V. Verselis, B. Eghbali, and D. C. Spray.** Voltage-dependent gap junction channels are formed by connexin32, the major gap junction protein of rat liver. *Biophys. J.* 59: 920–925, 1991.
28. **Moreno, A. P., B. Eghbali, and D. C. Spray.** Connexin32 gap junction channels in stably transfected cells: unitary conductance. *Biophys. J.* 60: 1254–1266, 1991.
29. **Moreno, A. P., B. Eghbali, and D. C. Spray.** Connexin32 gap junction channels in stably transfected cells. Equilibrium and kinetic properties. *Biophys. J.* 60: 1267–1277, 1991.
30. **Moreno, A. P., G. I. Fishman, E. C. Beyer, and D. C. Spray.** Voltage dependent gating and single channel analysis of heterotypic gap junction channels formed of Cx45 and Cx43. In: *Progress in Cell Research. Gap Junctions.* Amsterdam: Elsevier. In press.
31. **Moreno, A. P., G. I. Fishman, and D. C. Spray.** Kinetic analysis of single gap junction channels: use of communication-deficient cells (SKHep1) (Abstract). *Biophys. J.* 61: A505, 1992.
32. **Moreno, A. P., G. I. Fishman, and D. C. Spray.** Phosphorylation shifts unitary conductance and modifies voltage dependent kinetics of human connexin43 gap junction channels. *Biophys. J.* 62: 51–53, 1992.
33. **Moreno, A. P., M. B. Rook, G. I. Fishman, and D. C. Spray.** Gap junction channels: distinct voltage-sensitive and insensitive conductance states. *Biophys. J.* 67: 113–119, 1994.
34. **Moreno, A. P., J. C. Saez, G. I. Fishman, and D. C. Spray.** Human connexin43 gap junction channels. Regulation of unitary conductances by phosphorylation. *Circ. Res.* 74: 1050–1057, 1994.
35. **Neyton, J., and A. Trautmann.** Single-channel currents of an intercellular junction. *Nature Lond.* 317: 331–335, 1985.
36. **Nicholson, B. J., T. Suchyna, L. X. Xu, P. Hammernick, F. L. Cao, C. Fourtner, L. C. Barrio, and M. V. L. Bennett.** Divergent properties of different connexins expressed in *Xenopus* oocytes. In: *Progress in Cell Research. Gap Junctions,* edited by J. E. Hall, G. A. Zampighi, and R. M. Davies. Amsterdam: Elsevier, 1993, vol. 3, p. 3–13.
37. **Rubin, J. B., V. K. Verselis, M. V. Bennett, and T. A. Bargiello.** Molecular analysis of voltage dependence of heterotypic gap junctions formed by connexins 26 and 32. *Biophys. J.* 62: 183–193, 1992.
38. **Spray, D. C., A. L. Harris, and M. V. L. Bennett.** Voltage dependence of junctional conductance in early amphibian embryos. *Science Wash. DC* 204: 432–434, 1979.
39. **Spray, D. C., A. L. Harris, and M. V. Bennett.** Equilibrium properties of a voltage-dependent junctional conductance. *J. Gen. Physiol.* 77: 77–93, 1981.
40. **Spray, D. C., A. P. Moreno, B. Eghbali, M. Chanson, and G. I. Fishman.** Gating of gap junction channels as revealed in cells stably transfected with wild type and mutant connexin cDNAs. *Biophys. J.* 62: 48–50, 1992.
41. **Steinberg, T. H., R. Civitelli, S. T. Geist, A. J. Robertson, R. D. Veenstra, H.-Z. Wang, P. M. Warlow, E. Hick, J. G. Laing, and E. C. Beyer.** Connexin43 and connexin45 form gap junctions with different molecular permeabilities in osteoblastic cells. *EMBO J.* 13: 744–750, 1994.
42. **Veenstra, R. D., H. Z. Wang, E. C. Beyer, and P. R. Brink.** Differential permeability of connexin-specific gap junctions to fluorescent tracers (Abstract). *Biophys. J.* 64: A235, 1993.
43. **Veenstra, R. D., H. Z. Wang, E. M. Westphale, and E. C. Beyer.** Multiple connexins confer distinct regulatory and conductance properties of gap junctions in developing heart. *Circ. Res.* 71: 1277–1283, 1992.
44. **White, R. L., D. C. Spray, A. C. Campos de Carvalho, B. A. Wittenberg, and M. V. Bennett.** Some electrical and pharmacological properties of gap junctions between adult ventricular myocytes. *Am. J. Physiol.* 249 (*Cell Physiol.* 18): C447–C455, 1985.
45. **Wilders, R., and H. J. Jongsma.** Limitation of the dual voltage clamp method in assaying conductance and kinetics of gap junction channels. *Biophys. J.* 63: 942–953, 1992.
46. **Yancey, S. B., S. A. John, R. Lal, B. J. Austin, and J. P. Revel.** The 43-kDa polypeptide of heart gap junctions: immunolocalization, topology, and functional domains. *J. Cell Biol.* 108: 2241–2254, 1989.